PROTEINS: Structure, Function, and Genetics 8:23–29 (1990)

Protein Stability and Electrostatic Interactions Between Solvent Exposed Charged Side Chains

Mikael Akke and Sture Forsén
Physical Chemistry 2, Lund University, S-221 00 Lund, Sweden

ABSTRACT **To investigate the contribution to protein stability of electrostatic interactions between charged surface residues, we have studied the effect of substituting three negatively charged solvent exposed residues with their side-chain amide analogs in bovine calbindin D_{9k}—a small (M_r 8,500) globular protein of the calmodulin superfamily. The free energy of urea-induced unfolding for the wild-type and seven mutant proteins has been measured. The mutant proteins have increased stability towards unfolding relative to the wild-type. The experimental results correlate reasonably well with theoretically calculated relative free energies of unfolding and show that electrostatic interactions between charges on the surface of a protein can have significant effects on protein stability.**

Key words: urea induced unfolding, increased stability, site-directed mutagenesis, calbindin D_{9k}

INTRODUCTION

The understanding of protein folding is one of the most important goals in molecular biology. It is widely accepted that the hydrophobic effect provides the major part of the free energy of folding in aqueous systems, whereas the contributions of more specific interactions remain to be clarified. The importance of various factors to the stability of proteins can be assessed by equilibrium unfolding measurements. Such studies provide valuable experimental data, against which theoretical models can be checked. Site-specific mutagenesis offers the possibility to investigate systematically the effects of specific interactions in proteins, without relying on estimates from model compounds, and considerable progress is now being made towards the understanding of protein stability. The effects of creating a cavity in a protein,[1,2] perturbing hydrogen bonding patterns,[3] and of interactions with α-helix dipoles[4,5] have been addressed. Our group has recently reported on the effect of long-range electrostatic interactions on the calcium binding properties of calbindin D_{9k}—a small (M_r 8,500) globular protein of the calmodulin superfamily.[6] Here, we present a study on the contribution of electrostatic interactions between surface charges to the stability towards unfolding of the protein.

Bovine calbindin D_{9k} is a 75-residue calcium binding protein consisting of two "EF-hands" (helix-loop-helix motif), joined by a third loop. Calbindin D_{9k} does not have any cysteine residues. The calcium binding loops in the EF-hands are situated close together in the calcium loaded form[7] (Fig. 1). Calbindin has a high proportion of charged amino acid residues (10 Lys (K), 4 Asp (D), and 13 Glu (E)), the total charge at neutral pH being −7. The negatively charged residues are predominantly located around the calcium sites. In this study we focus on three residues located in the loop forming site I: E17, D19, and E26. The side chains of these residues do not take part in the actual liganding of the calcium ions but still play an important role in the calcium binding process.[6] In order to study their contribution to the overall stability towards unfolding, these residues were replaced by side-chain amide analogs (Glu→Gln [Q] and Asp→Asn [N]), so as to effectively neutralize the charges, while altering the side chain structure as little as possible. In addition to the single mutations, the three possible double mutations (E17Q + D19N, E17Q + E26Q, D19N + E26Q) and the triple mutation (E17Q + D19N + E26Q) were constructed. Thus, a complete set of seven mutant proteins was obtained. The calcium loaded wild-type form is only marginally denatured by 8 M urea, and is stable at temperatures up to 100°C. As we have recently shown,[8] the calcium free (apo) wild-type and mutant forms show reversible unfolding under the same conditions, following a two-state process, and refold upon addition of calcium ions.

EXPERIMENTAL PROCEDURES

The wild-type and mutant genes of the minor A form of bovine calbindin D_{9k} were synthesized, expressed in *Escherichia coli,* and purified as described

Received September 20, 1989; revision accepted January 23, 1990.

Address reprint requests to Dr. Sture Forsén, Department of Physical Chemistry 2, Lund University, P.O. Box 124, S-221 00 Lund, Sweden.

Mikael Akke's temporary address is: Department of Molecular Biology, Research Institute of Scripps Clinic, 10666 North Torrey Pines Road, La Jolla, California 92037.

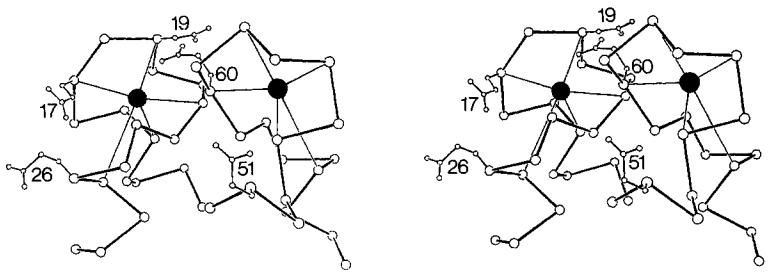

Fig. 1. Stereo view of the two calcium binding loops of calbindin D_{9k}. Residues E17, D19, and E26 are all located in loop I.

previously, [9,10] except that the urea-treatment step was replaced by heating to avoid deamidation of the protein.[11] The stability towards unfolding was measured by following the reversible urea-induced denaturation with circular dichroism spectroscopy. The experiments were performed on a JASCO J-500A spectropolarimeter, using a 1 mm water-jacketed cuvette thermostated at 25.0 (± 0.1)°C. The protein solutions contained 10–20 μM calbindin, 0.3 mM EDTA (ethylenediaminetetraacetic acid) and ultra-pure urea (Aristar, BDH) of concentrations varying from 0 to 7.96 M, dissolved in 20 mM PIPES (1,4-piperazinebis[ethanesulfonic acid])/KOH buffer at pH 7.0. The ellipticity at 222 nm was measured at increasing urea concentations, thereby monitoring the denaturation of the α-helices.

Following several previous studies,[12] we make the assumption that the free energy of unfolding is a linear function of the urea concentration:

$$\Delta G = \Delta G_0 + A \cdot c$$

where ΔG is the free energy of unfolding at urea concentration c, ΔG_0 is the free energy of unfolding at zero urea concentration, and A is the linear coefficient. Using this expression we fit the parameters ΔG_0 and A directly to the experimental data (the normalized ellipticity and the urea concentration), using standard non-linear least-squares fit routines[13] and the following relationships:

$$\Theta_{obs} = (\Theta_N + K_U\Theta_U)/(1 + K_U),$$
$$K_U = \exp\{-(\Delta G_0 + A \cdot c)/RT\}$$

where Θ_{obs} is the observed ellipticity at urea concentration c, and Θ_N and Θ_U denote the ellipticity of the native protein and the unfolded protein, respectively. K_U is the equilibrium constant for the unfolding process, R is the gas constant, and T is the absolute temperature.

RESULTS

The free energy of unfolding, $\Delta G_{N\to U}$, for the apo form of the wild-type and mutant proteins is presented as a function of urea concentration in Figure 2. All seven mutant proteins have increased stability relative to the wild-type in the unfolding transition region. In view of the uncertainties involved in extrapolating to zero urea concentration, the relative stabilities among similar mutant proteins are best assessed by taking the difference in stability at an urea concentration closer to the transition midpoints of the mutants.[1] Neither the values obtained for the free energy of unfolding at 5.0 M urea nor the transition midpoint concentrations (Table I) reveal any immediate relationship between the number of charges eliminated and the relative stabilities.

MODEL CALCULATIONS AND DISCUSSION

Detailed structural information is a prerequisite for accurately modeling the free energy of processes occurring in proteins. Microscopic calculations of the free energy of such processes as ionization of acidic groups in proteins,[14] mutations of side chains in proteins,[15] and binding of inhibitors to proteins[16] have been performed. Many of these agree very well with experimental data. In order to discuss what factors underlie the differences in stability among the wild-type and mutant calbindins, one obviously would like to know the three-dimensional structures of these proteins, both in their calcium loaded and apo forms. The crystal structure of the calcium loaded wild-type has been published,[7] but the struc-

TABLE I. Free Energy of Unfolding*

Mutant	$\Delta G_{N\to U}$(5 M)† (kJ/mol)	C_m (M)	$\Delta\Delta G_{N\to U}$(wt→μ) (kJ/mol)
E17Q	2.8 ± 0.2	5.6	1.6
D19N	4.3 ± 0.3	5.9	3.0
E26Q	1.6 ± 0.2	5.3	0.4
E17Q+D19N	6.2 ± 0.3	6.2	5.0
E17Q+E26Q	2.3 ± 0.2	5.5	1.0
D19N+E26Q	3.4 ± 0.2	5.8	2.2
E17Q+D19N +E26Q	5.1 ± 0.3	6.1	3.8
Wild-type	1.2 ± 0.2	5.3	—

*Free energy of unfolding at 5 M urea, $\Delta G_{N\to U}$(5 M). Urea concentration at the transition midpoint, C_m. Relative free energy of unfolding, $\Delta\Delta G_{N\to U}(wt\to\mu) = \Delta G_{N\to U}(\mu) - \Delta G_{N\to U}(wt)$. These values were obtained from the experimentally fitted functions $\Delta G = \Delta G_0 + A \cdot c$ (see Figure 2).
†(± standard deviation).

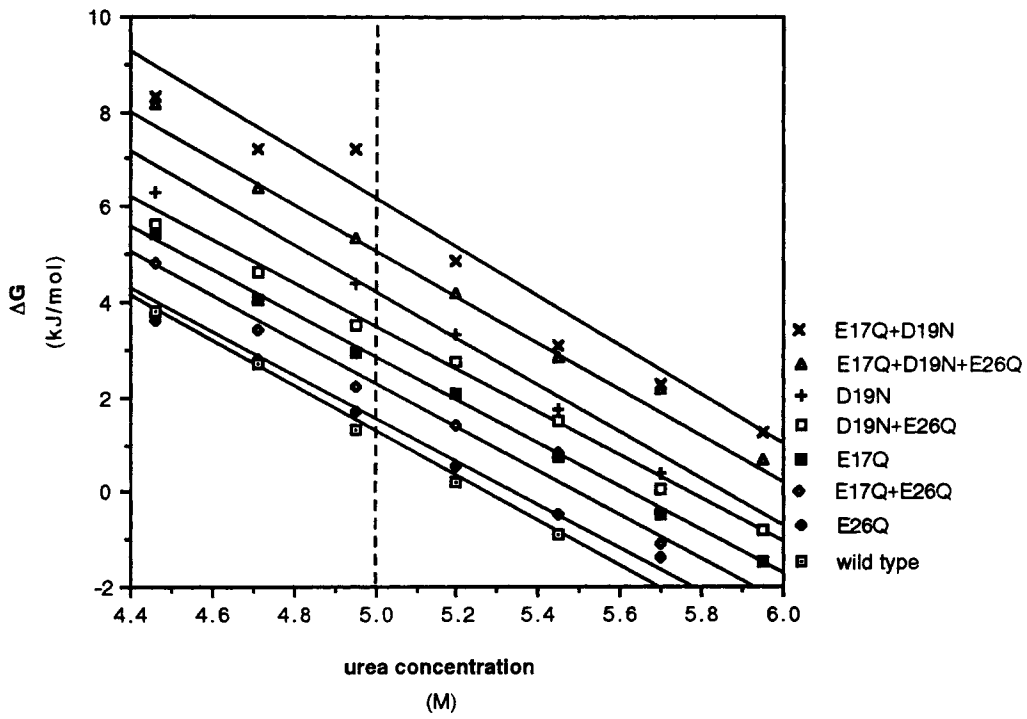

Fig. 2. Experimental data and the fitted functions $\Delta G = \Delta G_0 + A \cdot c$ (see the text) for the wild-type and the mutant proteins. Note that this enlarged view only shows a part of the data points used to fit the parameters of the linear function to the experimental data. The resulting functions are—

E17Q+D19N:	$\Delta G = 31.8\ kJ \cdot mol^{-1} - 5.12\ kJ \cdot mol^{-1} \cdot M^{-1} \cdot c$
E17Q+D19N+E26Q:	$\Delta G = 29.4\ kJ \cdot mol^{-1} - 4.86\ kJ \cdot mol^{-1} \cdot M^{-1} \cdot c$
D19N:	$\Delta G = 28.8\ kJ \cdot mol^{-1} - 4.90\ kJ \cdot mol^{-1} \cdot M^{-1} \cdot c$
D19N+E26Q:	$\Delta G = 26.0\ kJ \cdot mol^{-1} - 4.51\ kJ \cdot mol^{-1} \cdot M^{-1} \cdot c$
E17Q:	$\Delta G = 25.6\ kJ \cdot mol^{-1} - 4.55\ kJ \cdot mol^{-1} \cdot M^{-1} \cdot c$
E17Q+E26Q:	$\Delta G = 25.3\ kJ \cdot mol^{-1} - 4.60\ kJ \cdot mol^{-1} \cdot M^{-1} c$
E26Q:	$\Delta G = 24.4\ kJ \cdot mol^{-1} - 4.56\ kJ \cdot mol^{-1} \cdot M^{-1} \cdot c$
Wild-type:	$\Delta G = 25.0\ kJ \cdot mol^{-1} - 4.75\ kJ \cdot mol^{-1} \cdot M^{-1} \cdot c$

ture of apo-calbindin has not yet been determined. Two-dimensional ^1H nuclear magnetic resonance (NMR) studies of the apo form[17] show that the secondary structure and the global fold are very similar to those of the calcium form.[18] However, the NMR data indicate that the mini β-sheet between the two calcium binding loops, while clearly present, is perturbed in the solution structure of the apo form.[17] This suggests that there may be small, but distinct conformational changes upon calcium release (possibly a separation of the loops). Since the residues substituted in this study are all located in the same loop, a separation of the loops would affect the electrostatic interactions of these residues in the same direction. Although the lack of detailed structural information dicourages the use of more accurate model calculations, we can nonetheless achieve a fair understanding of the basis for the differences in stability among the mutant calbindins, since to a first approximation the structure changes upon calcium binding can be expected to be similar in all mutant proteins. We thus take the structure of the apo form to be identical to the calcium loaded form, and this is one of the basic assumptions in the model calculations outlined below.

To account for the relative stabilities we consider the following thermodynamic cycle:

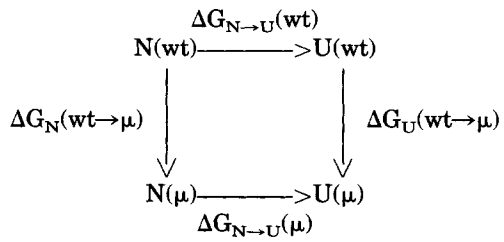

where N stands for the native state of the protein and U for the unfolded state. The wild-type protein is denoted wt and the mutant μ. The difference in the free energy of unfolding between the particular mutant and the wild-type is given by

$$\Delta\Delta G_{N\rightarrow U}(wt\rightarrow\mu) = \Delta G_{N\rightarrow U}(\mu) - \Delta G_{N\rightarrow U}(wt)$$

This can alternatively be expressed as the difference in free energy of a fictitious mutation process taking place in the unfolded and native state:

$$\Delta\Delta G_{N\rightarrow U}(wt\rightarrow\mu) = \Delta G_{U}(wt\rightarrow\mu) - \Delta G_{N}(wt\rightarrow\mu) \quad (1)$$

The two terms of the right-hand side of Equation 1 can be divided further into separate terms dependent on the type of interaction. Such a division is somewhat arbitrary, but—as we will argue below—for the purpose of this study it suffices to separate the electrostatic free energy from the rest of the contributing terms, and express the change in free energy upon side chain substitution as

$$\Delta G(wt\rightarrow\mu) = \Delta G_{elstat}(wt\rightarrow\mu) + \Delta G_{other}(wt\rightarrow\mu)$$

where ΔG_{elstat} refers to the intra-protein electrostatic interactions, and the interactions between charges on the protein and the solvent. ΔG_{other} refers to all other changes in free energy of non-electrostatic origin.

The substitutions involve only functional groups of side chains that are exposed to the surrounding solvent. Assuming that the conformations of the mutant proteins do not differ greatly from the wild-type, it seems plausible that there are no significant changes in van der Waals-type interactions, and that the exposure of the side chains to the solvent is not altered. That is, $\Delta G_{other}(wt\rightarrow\mu) = 0$ for both the native and unfolded state. Given these approximations, Equation 1 reduces to

$$\Delta\Delta G_{N\rightarrow U}(wt\rightarrow\mu) = \Delta G_{U,elstat}(wt\rightarrow\mu) - \Delta G_{N,elstat}(wt\rightarrow\mu) \quad (2)$$

Thus the differences in stability towards unfolding are predicted to be dependent on the changes in the electrostatic free energy that are caused by the mutations.

Macroscopic continuum models have been used rather successfully in describing long-range electrostatic interactions (for reviews see, e.g., references 19–21), especially when the shape of the molecule is taken into account as in finite difference methods.[22,23] Simple but widely used approaches treat the protein and its surroundings as a uniform dielectric medium, or apply a distance dependent dielectric.[19–21] Effects of the electrostatic potential on rates of enzyme catalysis[22] and pK_a shifts[24–26] have previously been presented.

In order to simplify the evaluation of the electrostatic free energy we consider the monopole terms only, and disregard all higher multipoles. Then, $\Delta G_{elstat}(wt\rightarrow\mu)$ is equal to the energy of the charge on the residue to be substituted. This energy includes all pairwise interaction energies, and the Born energy of the charge. Using a unifrom dielectric model for both the native and the unfolded state, and taking the dielectric constant to be the same for both states, the Born energy of the charge cancels in Equation 2, so that $\Delta G_{elstat}(wt\rightarrow\mu)$ is simply given by the Coulomb energy:

$$\Delta G_{elstat} = \sum_{k}\sum_{l}\frac{Q_k Q_l e^2}{4\pi\epsilon_0\epsilon_r r_{kl}} \quad (3)$$

where k denotes the charge(s) to be "neutralized," l denotes all other charges, Q is the charge (in units of e), e is the elementary charge, ϵ_0 is the vacuum permittivity, ϵ_r is the dielectric constant, and r_{kl} is the distance between charges k and l. For the triple and double mutants, each interaction is counted only once (i.e., ΔG_{elstat} for the second charge is evaluated in the system where the first charge has already been removed, and ΔG_{elstat} for the third charge where the first and the second charges have been removed).

$\Delta G_{N,elstat}(wt\rightarrow\mu)$ is estimated from Equation 3, using an effective dielectric constant, ϵ_r, of $78.r_{kl}$ is assigned the arithmetic mean value of the distance between the charges, calculated from a 124 ps molecular dynamics (MD) simulation of the calcium form of calbindin in water.[27] We use data from the MD simulation, rather than from the x-ray crystal structure, for the following reason: The MD simulation, which was started from the crystal structure, provides mean values of the distances, and should be free of any interactions, e.g., salt bridges, that are particular to the crystal state. (This argument is supported by a recent and more detailed study.[28]) The electrostatic screening by ions in the solution is taken into account by multiplying each term in Equation 3 by $\exp(-\kappa r_{kl})$, where κ is the Debye-Hückel screening parameter. κ is set to 0.0364 $Å^{-1}$, as calculated from the composition of the protein solutions.

For the unfolded state the calculation of r_{kl} is less straightforward. What is usually called the "unfolded state" probably consists of a large set of conformations with similar energies. This presents a major obstacle to the calculation of the most probable distance between any two points in an unfolded protein. Here, we estimate $\Delta G_{U,elstat}(wt\rightarrow\mu)$ from the following arbitrary model: For interactions between charges that are three residues apart or closer, we consider an extended polypeptide backbone with the side chains in staggered conformations, and take r_{kl} to be the mean value of the longest and shortest distances possible. For charges that are further apart, we calculate r_{kl} from the "freely rotating chain" model.[29] The distance between two joints in the "freely-rotating chain" model is given by $r_{kl} = \{nl^2[n(1-\alpha)(1+\alpha) - 2\alpha(1-\alpha^n)]/[n(1-\alpha)^2]\}^{1/2}$. The length of each chain segment is set equal to the $C^\alpha(i)-C^\alpha(i+1)$ distance in a rigid peptide unit, $l = 3.8$ Å (i.e. the C^α-atoms are the joints of the chain); n is the number of chain segments; α is the cosine of the angle around which the

TABLE II. Calculated and Experimental Values of $\Delta\Delta G_{N\to U}(wt\to\mu)$*

	Uniform			Tanford-Kirkwood		Experimental
	$\Delta G_U(wt\to\mu)$† (kJ·mol^{-1})	$\Delta G_N(wt\to\mu)$ (kJ·mol^{-1})	$\Delta\Delta G_{N\to U}(wt\to\mu)$ (kJ·mol^{-1})	$-\Delta G_N(wt\to\mu)$ (kJ·mol^{-1})	$\Delta\Delta G_{N\to U}(wt\to\mu)$ (kJ·mol^{-1})	$\Delta\Delta G_{N\to U}(wt\to\mu)$ (kJ·mol^{-1})
E17Q	0.04	4.64	4.68	4.27	4.31	1.6
D19N	−0.54	8.11	7.57	8.13	7.59	3.0
E26Q	−0.23	1.67	1.44	−0.70	−0.93	0.4
E17Q+D19N	1.09	11.77	12.86	11.45	12.54	5.0
E17Q+E26Q	0.10	3.88	3.98	0.31	0.41	1.0
D19N+E26Q	−0.36	9.18	8.82	6.95	6.59	2.2
E17Q+D19N +E26Q	1.56	10.40	11.96	7.00	8.56	3.8

*Calculated values of $\Delta G_U(wt\to\mu)$, $-\Delta G_N(wt\to\mu)$ and $\Delta\Delta G_{N\to U}(wt\to\mu)$, and experimental value of $\Delta\Delta G_{N\to U}(wt\to\mu)$.
†$\Delta G_U(wt\to\mu)$ is calculated using the uniform model only. This value is used in the calculation of $\Delta\Delta G_{N\to U}(wt\to\mu)$ for both the Tanford-Kirkwood model and the uniform model.

chain is allowed to rotate. The angle is set equal to 40° (based on standard polypeptide backbone geometry). The charges are assigned to the C^α-atoms. It should be remarked that the "freely rotating chain" model is not consistent with the presence of charges along the chain. However, it provides a means to get a rough estimate of the electrostatic interactions in the unfolded state (favoring the "random chain" model over the "molten globule"). The resulting values for $\Delta G_U(wt\to\mu)$ and $\Delta G_N(wt\to\mu)$ (Table II) show that the effects of substitutions are less dramatic for the electrostatic free energy of the unfolded state than for that of the native state. The amino acid sequence of calbindin D_{9k} is such that sequentially close interactions involving the substituted residues largely cancel in any extended chain model: E17 is surrounded by K16 and D19; D19 by K16, E17, and K25; E26 by K25 and E27. The values of $\Delta\Delta G_{N\to U}(wt\to\mu)$ calculated using Equation 3, as outlined above, are compared with the experimental data in Table II and Figure 3. There is a clear correlation between the calculated and experimental points.

The theoretical calculations can be extended so that the dielectric boundary between the protein and the solvent is included. Here, we have used the Tanford-Kirkwood model[30] to calculate the interaction energies of the charges in the native state. The Tanford-Kirkwood model and modified versions of it have been shown to reproduce the titration behaviour of globular proteins with reasonable accuracy.[19–21] In this model the protein is represented as a homogeneous low-dielectric sphere, with all of its charges located on the surface, surrounded by a high-dielectric medium. The representation of the protein as a sphere is a quite reasonable approximation. In the crystalline state,[7] calbindin is a prolate ellipsoid with axes 25 Å and 30 Å—which is in good agreement with the MD simulation.[27] The longest distance between two surface charges, as calculated from the MD simulation, is exactly (± 0.05 Å), equal to the diameter of the resulting model sphere. These charges are located at roughly diametrically opposite points in the crystal structure. The radius of the sphere is calculated from the radius of gyration, r_G, as obtained from the MD simulation. The radius of a homogeneous sphere is given by $r = r_G/(0.6)^{0.5}$. Accordingly, r_p = 13.8 Å. The ion exclusion radius is set to 15 Å. The dielectric constant of the protein sphere is set to 2, and the dielectric constant of the surrounding solvent is set to 78. All other parameters are the same as, or deduced from, those in the uniform model.

Methods to deal with the Born energy of a charge on the surface of a sphere have been worked out.[31] A corresponding model for the unfolded state that accounts for the dielectric inhomogeneity seems less readily attainable on the computational level chosen for this preliminary study. Such a model is required for a rigorous analysis, since the Born energy has to be treated explicitly when the dielectric function is not the same in the models of the two states. However, it has been argued that the Born energy is not extremely important for charged groups on the surface of the protein,[19] and that this should be the reason for the success of the Tanford-Kirkwood model in predicting protein titration curves. We have simply taken the Born energy to be the same for the unfolded and the native state, and modeled the unfolded state as before. The resulting $\Delta\Delta G_{N\to U}(wt\to\mu)$ values are listed in Table II. As shown in Figure 3, the Tanford-Kirkwood model gives a better correlation with the experimental values than the uniform model; in particular, the calculated values follow the same trend as the experimental ones.

The difference between the results of the two models can be rationalized as follows: In the Tanford-Kirkwood model, each charge interacts not only directly with the other charges, but also with the polarization of the solvent induced by the other charges. Depending on the locations of charges around a particular charge site, the Tanford-Kirkwood energy may thus deviate more or less from that calculated with the uniform model—as is seen for E26Q (Fig. 3).

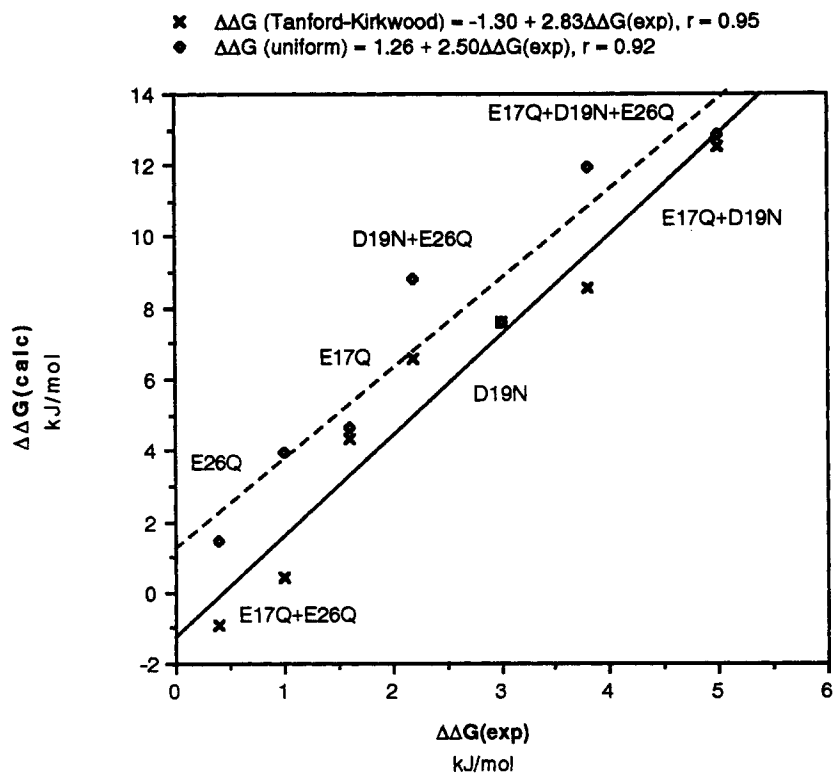

Fig. 3. The values of $\Delta\Delta G_{N\rightarrow U}(wt\rightarrow\mu)$ for the uniform dielectric model, and the Tanford-Kirkwood model, ΔΔG(calc), plotted against the corresponding experimental values, ΔΔG(exp) (broken and full line, respectively).

The calculations overestimate the electrostatic free energies of unfolding. We argue that on the basis of the nature of the system we describe, the correlation of the experimental and theoretical data is more important than absolute agreement. This is so for the following two reasons: 1) The unfolded state may be more compact than what is implied by the freely rotating chain model. It appears likely that interactions between sequentially distant charges have less importance in a more flexible, unfolded state than in the folded state (where they may be fixed at a close distance from each other), whereas interactions between sequentially close charges necessarily will be important. The actual value of the electrostatic energy for a certain charge in the unfolded state will vary with the dimensions and compactness of the unfolded protein, but the leading contributions from the sequentially close interactions should be caught by the model used in this study, and be reflected by the correlation of the experimental and theoretical data. 2) The structure of the apo protein is not known in detail, and it may be possible that the two calcium binding loops are more separated in this form than in the calcium loaded form, which is used as a model in the present study. It appears likely that this would result in lower magnitudes for the free energies of the deleted charges, since both loops have a negative net charge. The strongest interactions (those within the "mutated" loop) would still be of the same magnitude as in the calcium loaded form, however, and therefore the trend for the electrostatic free energies of the deleted charges would be largely unaffected. We have performed a crude test on the effect of such a separation by calculating the electrostatic free energies, using the uniform dielectric model, for a case where all distances between the deleted charges and charges in the second half of the protein have been increased by 5 Å. This results in a roughly 50% decrease of the calculated electrostatic free energy, and also a slightly higher correlation coefficient (Data not shown.)

CONCLUSIONS

The present study shows that the electrostatic free energy is an important factor in determining the stability towards unfolding of apo-calbindin D_{9k}. It appears that even fairly crude models of the protein work well in explaining the experimental data. The results indicate that the contribution of electrostatic interactions between surface charges to the stability of proteins in general must be accounted for. A large number of proteins are found to have highly charged surface regions that in many cases have been shown

to be of functional importance.[6,32,33] Protein engineering designed to affect such functions by introducing or deleting charged residues clearly could also have marked effects on the stability of the protein.

ACKNOWLEDGMENTS

We thank P. Brodin and Dr. T. Grundström for the samples of mutant *E. coli,* and E. Thulin for technical excellence in purifying the proteins. Drs. O. Teleman and P. Ahlström are thanked for making available data from the MD simulation. Dr. H. Wennerström is thanked for valuable discussions. M.A. receives a graduate scholarship from the Crafoord Foundation, which is gratefully acknowledged.

REFERENCES

1. Kellis, J.T., Nyberg, K., Sali D., Fersht, A.R. Contribution of hydrophobic interactions to protein stability. Nature 333:784–786,1988.
2. Matsumura, M., Becktel, W.J., Matthews, B.W. Hydrophobic stabilization in T4 lysozyme determined directly by multiple substitutions of Ile3. Nature 334:406–410,1988.
3. Alber, T., Dao-pin, S., Wilson, K., Wozniak, J.A., Cook, S.P., Matthews, B.W. Contributions of hydrogen bonds of Thr 157 to the thermodynamic stability of phage T4 lysozyme. Nature 330:41–46,1987.
4. Nicholson, H., Becktel, W.J., Matthews, B.W. Enhanced protein thermostability from designed mutations that interact with α-helix dipoles. Nature 336:651–656,1988.
5. Sali, D., Bycroft, M., Fersht, A.R. Stabilization of protein structure by interaction of α-helix dipole with a charged side chain. Nature 335:740–743,1988.
6. Linse, S., Brodin, P., Johansson, C., Thulin, E., Grundström, T., Forsén, S. The role of protein surface charges in ion binding. Nature 335:651–652, 1988.
7. Szebenyi, D.M.E., Moffat, K. The refined structure of vitamin D-dependent calcium-binding protein from bovine intestine. J. Biol. Chem. 261:8761–8777,1986.
8. Wendt, B., Hofmann, T., Martin, S.R., Bayley, P., Brodin, P., Grundström, T., Thulin, E., Linse, S., Forsén, S. Effect of amino acid substitutions and deletions on the thermal stability, the pH stability and unfolding by urea of bovine calbindin D_{9k}. Eur. J. Biochem. 175:439–445,1988.
9. Brodin, P., Grundström, T., Hofmann, T., Drakenberg, T., Thulin, E., Forsén, S. Expression of bovine intestinal calcium binding protein from a synthetic gene in Eschericia coli and characterization of the product. Biochemistry 25: 5371–5377, 1986.
10. Linse, S., Brodin, P., Drakenberg, T., Thulin, E., Sellers, P., Elmdén, K., Grundström, T., Forsén, S. Structure-Function Relationships in EF-Hand Ca^{2+}-Binding Proteins. Protein Engineering and Biophysical Studies of Calbindin D_{9k}. Biochemistry 26:6723–6735,1987.
11. Chazin, W.J., Kördel, J., Thulin, E., Hofmann, T., Drakenberg, T., Forsén, S. Identification of an iso-aspartyl linkage formed upon deamidation of bovine calbindin D_{9k} and structural characterization by 2D ^1H NMR. Biochemistry 28:8646–8653, 1989.
12. Pace, C.N. Determination and analysis of urea and guanidine hydrochloride denaturation curves. Methods Enzymol. 131:266–280,1986.
13. Press, W.H., Flannery, B.P., Teukolsky, S.A., Vetterling, W.T. "Numerical Recipes." Cambridge University Press, New York, 1986.
14. Warshel, A., Sussman, F., King, G. Free energy of charges in solvated proteins: Microscopic calculations using a reversible charging process. Biochemistry 25:8368–8372, 1986.
15. Bash, P.A., Singh, U.C., Langridge, R., Kollman, P.A. Free energy calculations by computer simulation. Science 236: 564–568,1987.
16. Bash, P.A., Singh, U.C., Brown, F.K., Langridge, R., Kollman, P.A. Calculation of the relative change in binding free energy of a protein-inhibitor complex. Science 235: 574–576,1987.
17. Skelton, N.J., Kördel, J., Forsén, S., Chazin, W.J.C. in press J. Mol. Biol., 1989.
18. Kördel, J., Forsén, S., Chazin, W.J.C. ^1H NMR Sequential Resonance assignments, secondary structure and global fold in solution of the major (*trans* Pro43) form of bovine calbindin D_{9k}. Biochemistry 28:7065–7074,1989.
19. Harvey, S.C. Treatment of electrostatic effects in macromolecular modeling. Proteins 5:78–92,1989.
20. Warshel, A., Russell, S.T. Calculation of electrostatic interactions in biological systems and in solution. Q. Rev. Biophys. 17:283–422,1984.
21. Matthew, J.B. Electrostatic effects in proteins. Annu. Rev. Biophys. Chem. 14:387–417,1985.
22. Klapper, I., Hagstrom, R., Fine, R., Sharp, K., Honig, B. Focusing of electric fields in the active site of Cu-Zn superoxide dismutase: Effects of ionic strength and amino-acid modification. Proteins 1:47–59,1986.
23. Warwicker, J., Watson, H.C. Calculation of electric potential in the active site cleft due to α-helix dipoles. J. Mol. Biol. 157:671–679,1982.
24. Russell, A.J., Fersht, A.R. Rational modification of enzyme catalysis by engineering surface charge. Nature 328: 496–500,1987.
25. Sternberg, M.L.E. Hayes, F.R.F., Russell, A.J., Thomas, P.G., Fersht, A.R., Prediction of electrostatic effects of engineering of protein charges. Nature 330:86–88,1987.
26. Bashford, D., Karplus, M., Canters, G.W. Electrostatic effects of charge perturbations introduced by metal oxidation in proteins. A theoretical analysis. J. Mol. Biol. 203: 507–510,1988.
27. Ahlström, P., Teleman, O., Kördel, J., Forsén, S., Jönsson, B. A molecular dynamics simulation of bovine calbindin D_{9k}. Molecular structure and dynamics. Biochemistry 28: 3205–3211,1989.
28. Wendoloski, J.J., Matthew, J.B. Molecular dynamics effects on protein electrostatics. Proteins 5:313–321, 1989.
29. Cantor, C.R., Schimmel, P.R. "Biophysical Chemistry, Part III." Freeman, San Francisco: Freeman, 1980, p. 992.
30. Tanford, C., Kirkwood, J.G. Theory of protein titration curves. I. General equations for impenetrable spheres. J. Am. Chem. Soc. 79:5333–5339,1957.
31. Gilson, M.K., Rashin, A., Fine, R., Honig, B. On the calculation of electrostatic interactions in proteins. J. Mol. Biol. 184:503–516,1985.
32. Moore, J.M., Case, D.A., Chazin, W.J., Gippert, G.P., Havel, T.F., Powls, R., Wright, P.E. Three-dimensional solution structure of plastocyanin from the green alga *Scenedesmus obliquus*. Science 240:314–317,1988.
33. Getzoff, E.D., Tainer, J.A., Weiner, P.K., Kollman, P.A., Richardson, J.S., Richardson, D.C. Electrostatic recognition between superoxide and copper, zinc superoxide dismutase. Nature 306:287–290,1983.